Geological Magazine

www.cambridge.org/geo

Principal component analysis of textural characteristics of fluvio-lacustrine sandstones and controlling factors of sandstone textures

Dong-Yu Zheng[1] and Si-Xuan Wu[2]

[1]State Key Laboratory of Oil and Gas Reservoir Geology and Exploitation, Institute of Sedimentary Geology, Chengdu University of Technology, Chengdu, Sichuan, 610059, China and [2]Geology and Geophysics Program, Missouri University of Science and Technology, Rolla, MO, 65409, USA

Original Article

Cite this article: Zheng D-Y and Wu S-X (2021) Principal component analysis of textural characteristics of fluvio-lacustrine sandstones and controlling factors of sandstone textures. *Geological Magazine* **158**: 1847–1861. https://doi.org/10.1017/S0016756821000418

Received: 22 August 2020
Revised: 31 March 2021
Accepted: 20 April 2021
First published online: 21 May 2021

Keywords:
Sandstone texture; fluvio-lacustrine; PCA; depositional environments; provenance; Bogda Mountains; NW China

Author for correspondence:
Dongyu Zheng, Email: dzheng9295@126.com

Abstract

Textures are important features of sandstones; however, their controlling factors are not fully understood. We present a detailed textural analysis of fluvio-lacustrine sandstones and discuss the influences of provenance and depositional environments on sandstone textures. The upper Permian – lowermost Triassic Wutonggou sandstones in the Bogda Mountains, NW China, are the focus of this study. Sandstone thin-sections were studied by point counting and their textures were analysed using statistical and principal component analysis. Fluvial lithic, fluvial feldspathic, deltaic lithic, deltaic feldspathic, littoral lithic and littoral feldspathic sandstone were classified and compared. These comparisons indicate that lithic and feldspathic sandstones from the same depositional settings have significant differences in graphic mean, graphic standard deviation and roundness; in contrast, sandstones from different depositional settings but with similar compositions have limited differences in textures. Moreover, three principal components (PCs) are recognized to explain 75% of the total variance, of which the first principal component (PC1) can explain 44%. In bivariate plots of the PCs, sandstones can be distinguished by composition where lithic and feldspathic sandstones are placed in different fields of the plots along the axis of PC1. However, sandstones from different depositional settings overlap and show no clear division. These results indicate that provenance, mainly the source lithology, is the most significant controlling factor on sandstone texture, whereas the depositional environment has limited influence. This study improves our understanding of textural characteristics of fluvio-lacustrine sandstones and their controlling factors, and shows the potentiality of principal component analysis in sandstone studies.

1. Introduction

Sedimentary rocks record complex processes, including tectonic activities, weathering, transportation, deposition, diagenesis and their interactions on the Earth's surfaces (e.g. Suttner, 1974; Ingersoll *et al.* 1984; Johnsson, 1993). In order to understand these processes, the composition and textures of sedimentary rocks are widely studied. The provenance is accepted as the most determining control on the compositions of sedimentary rocks (Dickinson & Suczek, 1979; Johnsson, 1993; Garzanti, 2016), but the relationship between the provenance and textures is less discussed (Folk & Ward, 1957; Boulton, 1978; Arens *et al.* 2002). Moreover, many publications have attempted to relate the textural characteristics of sedimentary rocks to their depositional settings (e.g. Passega, 1957; Visher, 1969; Pettijohn *et al.* 1972; Barndorff-Nielsen, 1977; Folk, 1980; Boggs & Boggs, 2009). Different sandstone facies, especially the marine beach, dune and fluvial sandstones, have successfully been distinguished by their textural attributes (Folk & Ward, 1957; Friedman, 1962, 1967). However, scepticism of textural analysis demonstrates that textural attributes should be restricted to the purpose of description (Solohub & Klovan, 1970; Ehrlich & Full, 1987; Luplin & Hampson, 2020). Moreover, one problem in the previous textural studies is that only two textural parameters are plotted together, such as grain size versus sorting (Folk & Ward, 1957; Friedman, 1967), meaning that any multidimensional relationships cannot be interpreted. It is therefore intriguing to examine the relationship between textural features of fluvio-lacustrine sandstones and depositional environments under an *n*-dimensional space.

The textural analysis of upper Permian – lowermost Triassic fluvio-lacustrine Wutonggou low-order cycle (WTG-LC) sandstones in the Bogda Mountains of NW China provide a great opportunity to investigate the controlling factors on sandstone textures. High-resolution measured sections and the associated depositional environments of WTG-LC were documented (Yang *et al.* 2007, 2010), and detailed provenance studies of WTG-LC sandstones were conducted (Zheng, 2019; Zheng & Yang, 2020). Additionally, principal component analysis (PCA) is a powerful tool in geological studies to reduce dimension and classify samples

CAMBRIDGE UNIVERSITY PRESS

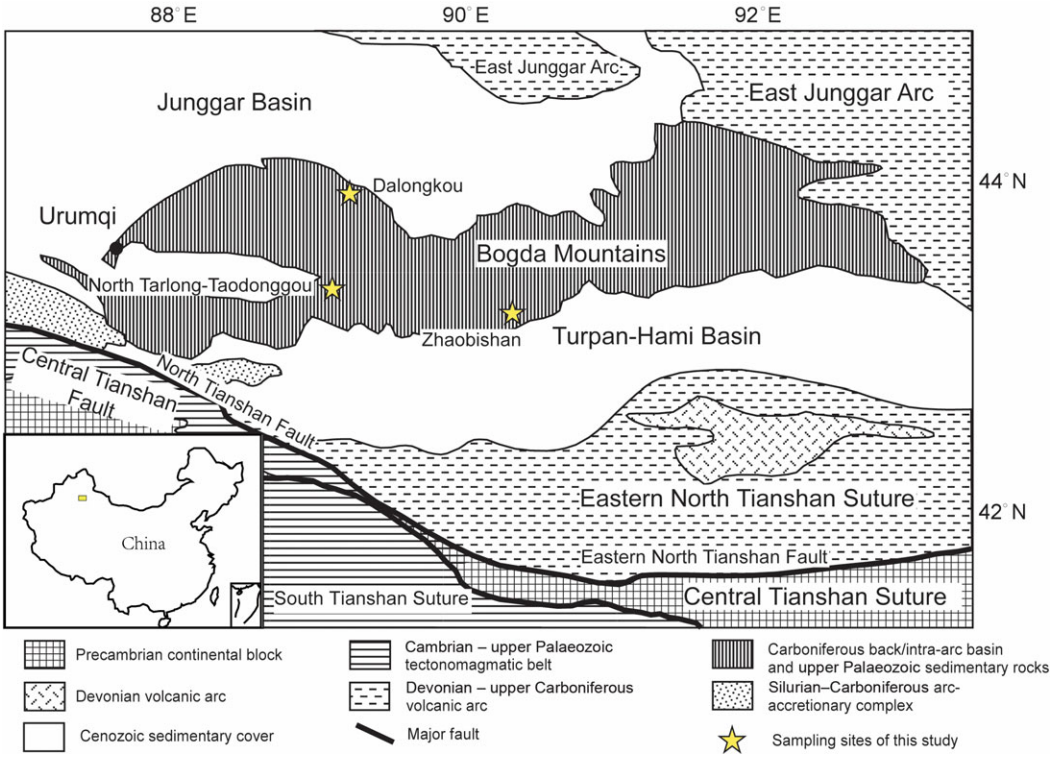

Fig. 1. (Colour online) Geological map of eastern Xinjiang, showing the locations of the Eastern North Tianshan Suture, Central Tianshan Suture, Bogda Mountains and measured sections. Modified from Xia *et al.* (2004).

(Davis & Sampson, 1986). We therefore focus on the WTG-LC sandstones to document their textural characteristics, compare textural characteristics of different facies using traditional and principal component analysis, and investigate the controlling factors on sandstone textures.

2. Geological background

This study examines the upper Permian – lowermost Triassic fluvio-lacustrine sandstones of WTG-LC exposed in the northern and southern foothills of the Bogda Mountains (Fig. 1). Sandstones from four sections, including the Zhaobishan, North Tarlong, Taodonggou and Dalongkou sections, are the focus of this study (Fig. 2). The Bogda Mountains is a giant E–W-directed anticline with Devonian–Quaternary sedimentary and igneous rocks, located between the Junggar Basin to the north and Turpan-Hami Basin to the south in NW China. Before the Mesozoic uplift (Shao *et al.* 2001; Greene *et al.* 2005), the Bogda Mountains was a part of the greater Turpan–Junggar basin, which was an intracontinental rift basin formed by regional dextral strike-slip (Shu *et al.* 2011) and included a series of grabens and half-grabens (Yang *et al.* 2010). The Bogda Mountains is bordered by the Eastern North Tianshan Suture to the south, which is an amalgamated complex produced by the subduction of the North Tianshan Ocean and the collision between the Junggar Plate and the Central Tianshan Suture (Xiao *et al.* 2004; Charvet *et al.* 2011). The felsic-intermediate volcanic and plutonic rocks of the Eastern North Tianshan Suture and sedimentary rocks of the local rift shoulders are interpreted as the main sources of the sandstones in WTG-LC (Guan, 2011; Zheng, 2019; Zheng & Yang, 2020).

The WTG-LC is an informal cyclostratigraphic unit that reflects an overall subhumid–humid climatic condition and a history of persistent uplifting of source regions (Yang *et al.* 2007, 2010; Thomas *et al.* 2011; Zheng & Yang, 2020). The WTG-LC correlates with the Wutonggou and Guodikeng formations (XBGMR, 1993; Fig. 3). This correlation is based on lithostratigraphy, biostratigraphy and cyclostratigraphy (Wartes *et al.* 2002; Yang *et al.* 2007, 2010). The chronostratigraphy in the Bogda Mountains is not well defined; the Permian–Triassic boundary is placed in a 90-m-thick interval in the North Tarlong Section (Yang *et al.* 2010). Based on the stratigraphic and petrofacies correlation, the Dalongkou, North Tarlong-Taodonggou and Zhaobishan sections were deposited in different grabens or half-grabens with their own drainage areas and depocentres (Yang *et al.* 2010; Zheng & Yang, 2020). During late Permian – Early Triassic time, the Dalongkou section mainly received felsic-intermediate volcanic rocks from the western Eastern North Tianshan Suture, and mudrocks and sandstones from the surrounding rift shoulders. The North Tarlong-Taodonggou sections received felsic-intermediate igneous rocks from the western Eastern North Tianshan Suture, and mudrocks and sandstones from the surrounding rift shoulders. The Zhaobishan section mainly received chert, quartzite and felsic-intermediate igneous rocks from the eastern Eastern North Tianshan Suture (Zheng & Yang, 2020).

Fluvial, deltaic and littoral-lakeplain facies are categorized in the WTG-LC, which are interpreted based on the lithology, sedimentary texture and structures, palaeontological information, stratal geometry and boundary relationships (Fig. 4). The fluvial facies include braided stream and meandering stream subfacies. The braided stream facies is categorized by an upwards-fining succession of low-relief erosional base, channel-fill conglomerate and/or conglomeratic sandstones, and bar sandstones. The meandering stream environment is recognized by a high-relief erosional base, an upwards-fining succession of channel-fill conglomerate and/or conglomeratic sandstones, point bar sandstone and overbank mudrocks. The deltaic facies consist of the upwards-coarsening and thickening succession from prodeltaic shale and siltstone to delta front sandstone and/or conglomerate in the lower part,

https://doi.org/10.1017/S0016756821000418 Published online by Cambridge University Press

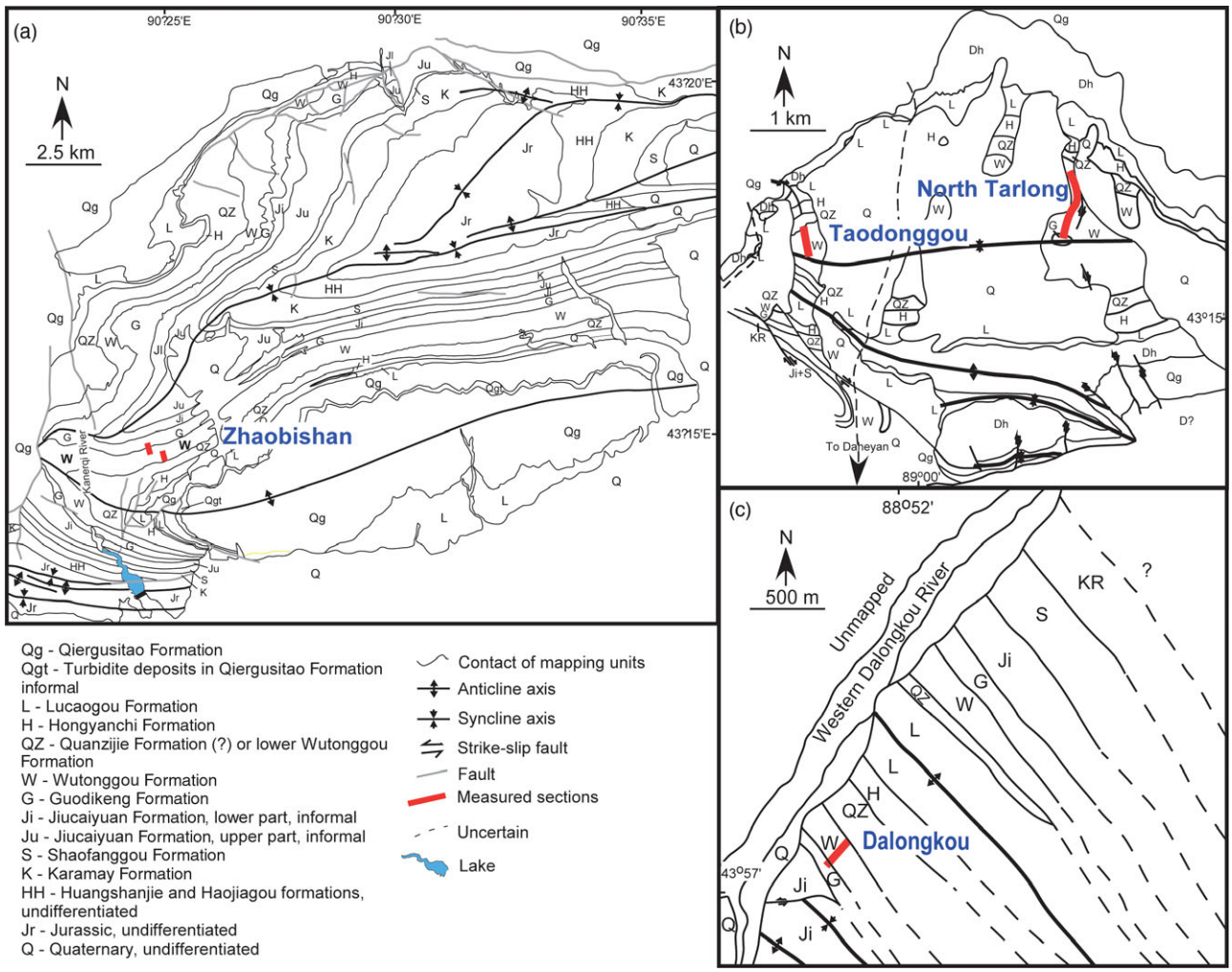

Fig. 2. (Colour online) Geological maps of (a) Zhaobishan, (b) North Tarlong-Taodonggou and (c) Dalongkou areas showing names and locations (red lines) of measured sections. Modified from Yang *et al.* (2010), Fredericks (2017) and Obrist-Farner & Yang (2017).

and distributary channel-fill and interdistributary deltaplain mudrock, sandstone, conglomerate and palaeosol in the upper part. The littoral-lakeplain facies is composed of the upwards-coarsening succession of sublittoral shale, littoral well-washed and laterally persistent sandstone and conglomerate in the lower part, and muddy to sandy palaeosol in the upper part.

3. Data and methodology

A total of 52 upper Permian – lowermost Triassic sandstones were collected from four sections in the northern and southern foothills of the Bogda Mountains that received sources from the Eastern North Tianshan Suture and rift shoulder sediments (Fig. 5; Zheng & Yang, 2020). The studied samples include four meandering stream point bar sandstones, seven braided stream bar sandstones, one braided stream channel sandstone, 15 delta front sandstones, and 25 littoral sandstones (Fig. 4). Sandstone samples were made into thin-sections to record their composition and textures by point counting. As matrix and cements are less than 1% of the total counting points in these sandstones, they were excluded from the following discussion. Additionally, 300 grains in each thin-section were counted with their grain type, size and roundness.

3.a. Sandstone grain composition

Point counting via Gazzi-Dickinson's method (Dickinson, 1970) counts sand-sized mineral crystals (grain size > 0.063 mm; $\Phi < 4$) within large lithic fragments as individual mineral grains to avoid the errors caused by grain-size effects (Ingersoll *et al.* 1984). Quartz (Q), feldspar (F) and lithic grains (L) were identified. Quartz includes monocrystalline crystals, polycrystalline and microcrystalline quartz aggregates. Feldspar consists of plagioclase (P) and potassium feldspar (K). Lithic grains are subdivided as volcanic (Lv) and sedimentary lithic grains (Ls). The Lv grains include felsic, microlitic and lathwork subtypes based on their textures. Felsic grains are interpreted as being derived from felsic igneous rocks; microlitic grains are interpreted as being derived from intermediate igneous rocks; and lathwork grains are interpreted as being derived from mafic igneous rocks (Dickinson, 1970; Marsaglia & Ingersoll, 1992). The Ls grains consist of mudrock, and scarce siltstone and sandstone fragments (Fig. 6). Based on this classification, the percentages of quartz, feldspar and lithic grains were calculated, and 22 feldspathic sandstones and 30 lithic sandstones were classified according to Dott's classification (Dott, 1964; Fig. 7; recalculated percentages in Table 1 and raw data in online Supplementary Table S1, available at http://journals.cambridge.org/geo; more details in Zheng & Yang, 2020).

https://doi.org/10.1017/S0016756821000418 Published online by Cambridge University Press

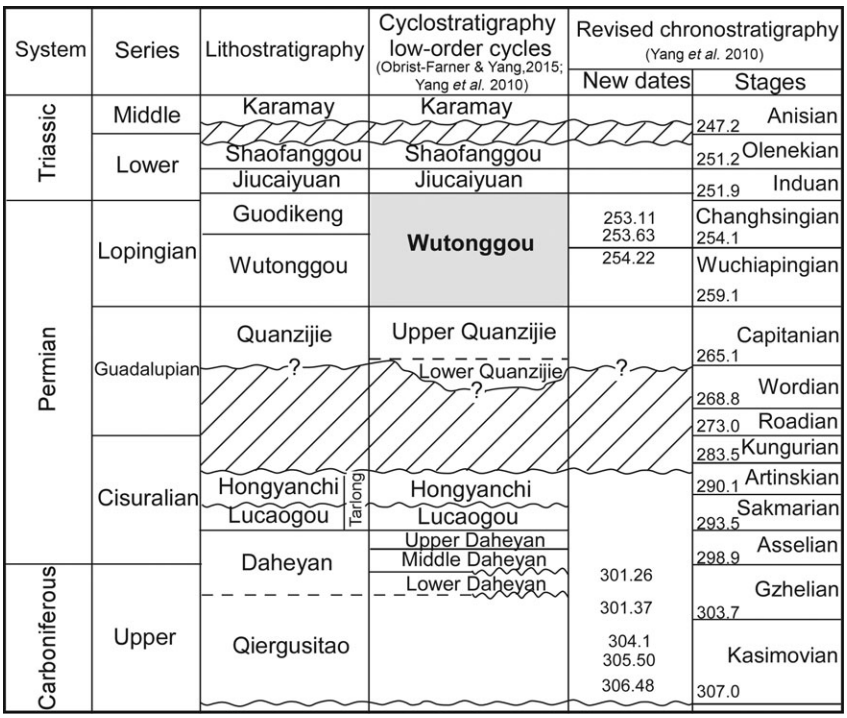

Fig. 3. (Colour online) Chrono-, litho- and cyclostratigraphy of upper Carboniferous – Middle Triassic strata in the Bogda Mountains. Wavy lines are major unconformities, dashed lines disconformities and hatched areas missing strata. The studied Wutonggou low-order cycle is shown in the shaded box. Modified from Yang *et al*. (2010) and Obrist-Farner & Yang (2015).

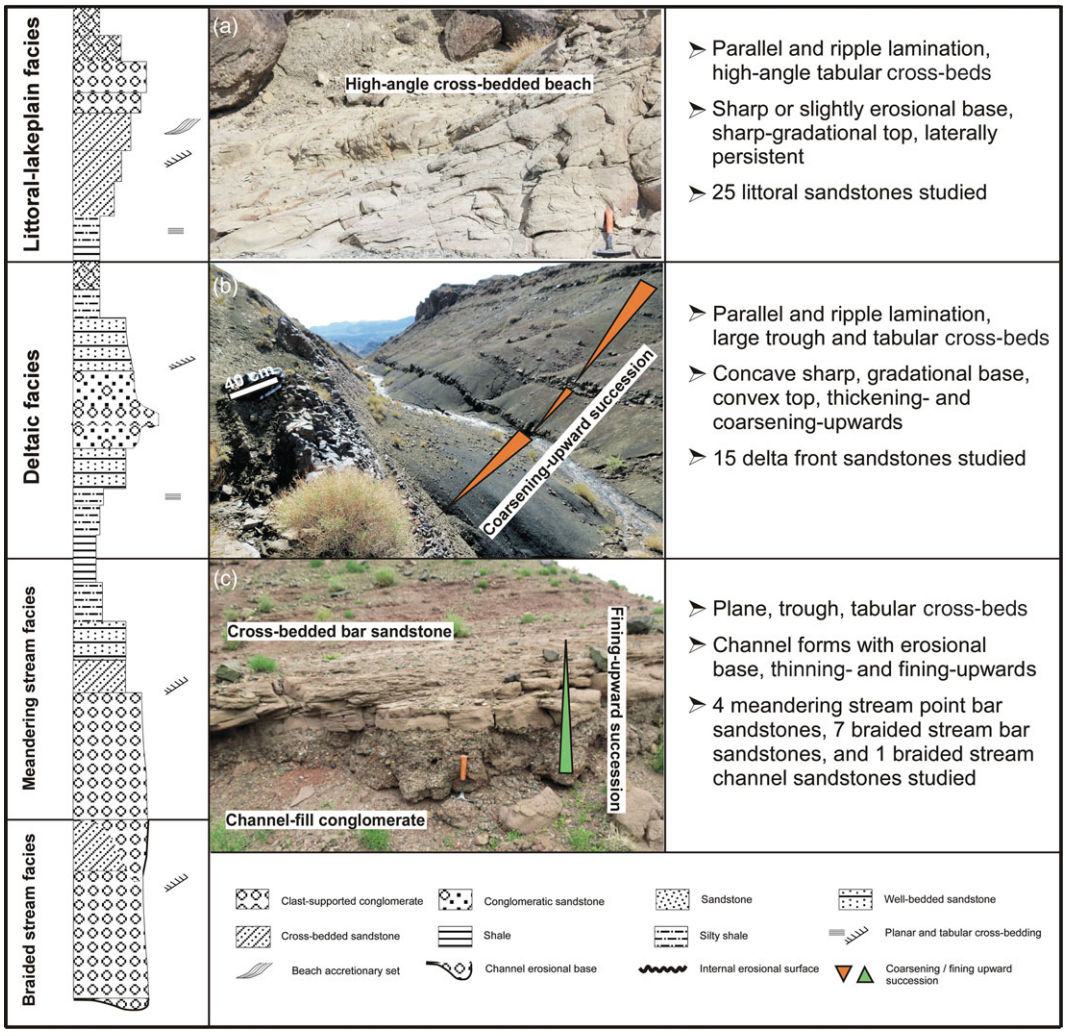

Fig. 4. (Colour online) Lithological columns and field photographs showing the lithology, sedimentary structure and stratal successions of major environmental facies: (a) littoral-lakeplain facies showing a high-angle beach accretionary set; (b) deltaic facies showing coarsening-upwards successions from shale to sandstone; and (c) fluvial facies showing a fining-upwards succession from channel-fill conglomerate to cross-bedded bar sandstone. See text and Yang *et al*. (2007, 2010) for detailed descriptions.

https://doi.org/10.1017/S0016756821000418 Published online by Cambridge University Press

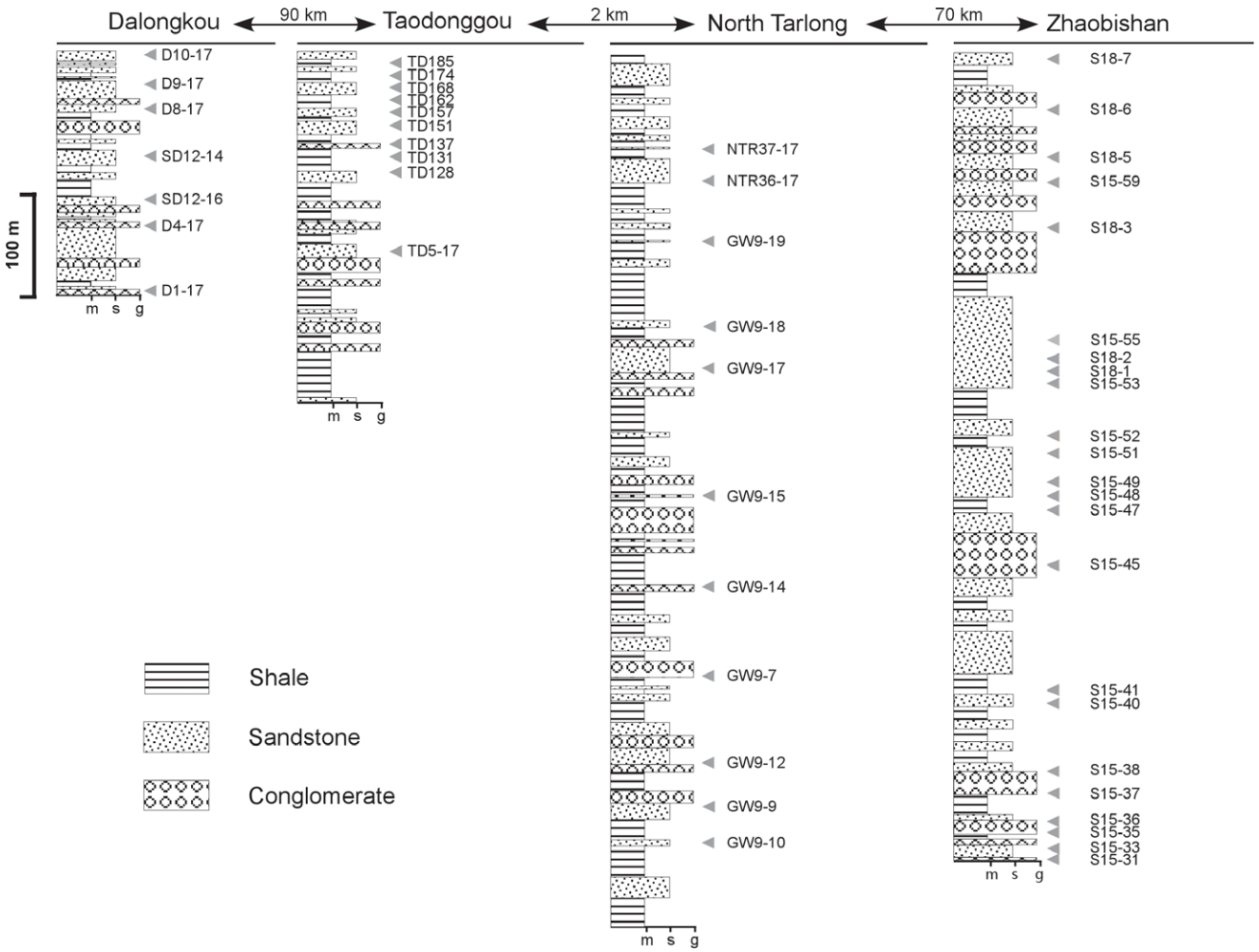

Fig. 5. (Colour online) Simplified lithological columns, showing section spatial relationships, sample numbers and locations.

Additionally, feldspathic sandstones consist of six fluvial feldspathic, four deltaic feldspathic and 12 littoral feldspathic sandstones; lithic sandstones include six fluvial lithic, 11 deltaic lithic and 13 littoral lithic sandstones (Fig. 7; Table 1).

3.b. Sandstone grain texture

For each thin-section, 300 grains have been investigated with their textural features. To better record the textural characteristics of the studied sandstones, in point counting of sandstone textures we followed Suttner's method (Suttner, 1974). Gazzi-Dickinson's method counts sand-sized individual grains, whereas Suttner's method counts phenocrysts as lithic fragments. We therefore investigate texture features of lithic fragments, excluding mineral crystals within the fragments. The grain-size statistical parameters, including the graphic mean (M_z), graphic standard deviation (SD), graphic skewness (SK_i) and graphic kurtosis (K_G), are calculated following formulae from Folk & Ward (1957). Verbal terms of the grain sizes, sorting, skewness and kurtosis are adapted from the Udden-Wentworth grain-size scale (Udden-Wentworth, 1922) and verbal limits in Folk & Ward (1957; Table 2). The grain roundness is estimated using the visual chart of roundness in Krumbein & Sloss (1951). In order to represent the degree of sandstone roundness, the percentages of angular (ANLR%) and rounded grains (RND%) have been calculated. Angular grains in this study include sub-angular and angular grains, and rounded grains consist of sub-rounded, rounded and well-rounded grains.

3.c. Principal component analysis

PCA is a multivariate analysis technique to investigate the hidden relationships among variables in a large dataset by dimension reduction and extraction of maximal information (Mardia *et al.* 1979). PCA transforms the multiple related variables into a small number of unrelated variables, which can explain the maximum amount of variance of the dataset. These unrelated variables are called principal components (PCs) and are sorted in the descending order of their explainable variance.

Let a sandstone contain m types of textural and compositional features. If there are n sandstones in the study, these data can be recorded in an $m \times n$ matrix, X, expressed as:

$$X = \begin{bmatrix} x_{1,1} & \cdots & x_{1,n} \\ \vdots & \ddots & \vdots \\ x_{m,1} & \cdots & x_{m,n} \end{bmatrix}.$$

By multiplying matrix X with its transposition X^T, the variance–covariance matrix can be obtained, which is expressed:

https://doi.org/10.1017/S0016756821000418 Published online by Cambridge University Press

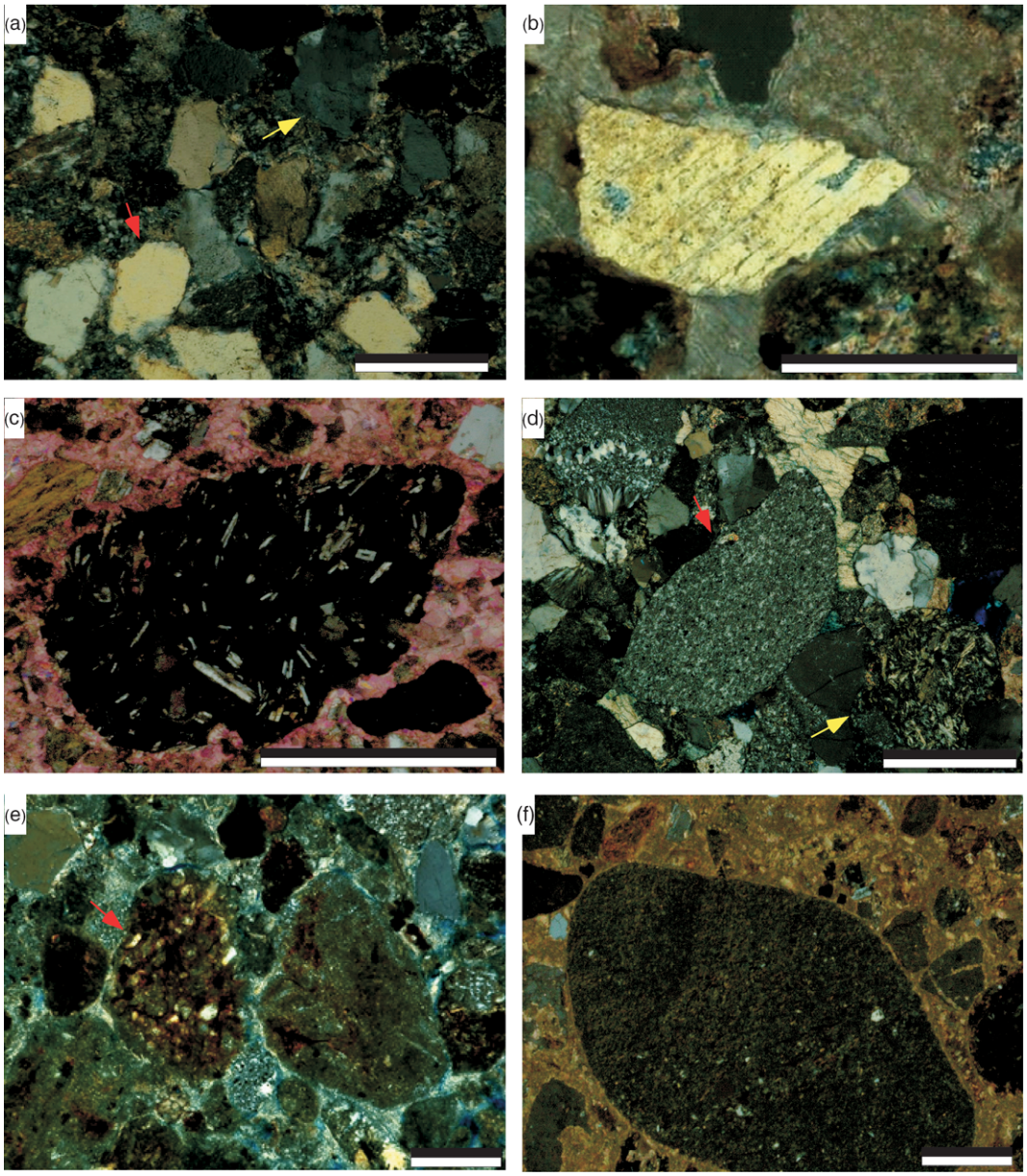

Fig. 6. (Colour online) Photomicrographs of Wutonggou low-order cycle sandstones. (a) Medium-sized, well sorted sandstones. The red arrow indicates a sub-rounded, medium-sand-sized monocrystalline quartz grain, and the yellow arrow indicates a sub-angular polycrystalline quartz. S15-40, deltaic lithic sandstones, lower Zhaobishan section. (b) Angular, coarse-sand-sized feldspar grains with visible parallel cleavages. (c) Rounded, coarse-sand-sized volcanic lithic grain with lathwork textures. (d) The red arrow indicates a rounded, coarse-sand-sized volcanic lithic grain with felsic to microlitic texture; the yellow arrow indicates a sub-rounded, coarse-sand-sized volcanic lithic grain with microlitic texture. (e) The red arrow indicates a coarse-sand-sized sandstone lithic grain. (f) Granule-sized rounded mudstone lithic grain. Micrographs were acquired are under cross-polarized light. Scale bar is 1 mm.

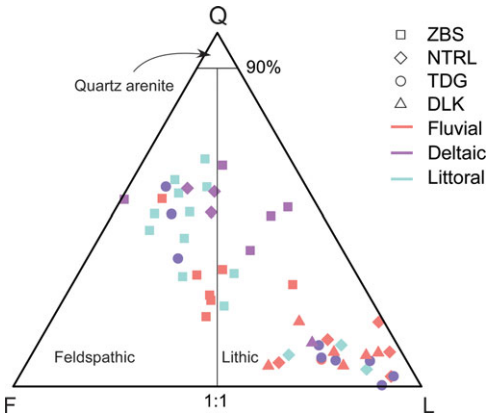

Fig. 7. (Colour online) Ternary diagrams showing composition of quartz, feldspar and lithic fragments and classification of Wutonggou low-order cycle sandstones. Feldspathic sandstones have the feldspar/lithic ratio > 1; lithic sandstones have the feldspar/lithic ratio < 1. The ternary template is modified from Dott (1964). See text for abbreviations.

$$XX^{T} = \begin{bmatrix} \sigma_{1,1}^2 & \sigma_{1,2}^2 & \cdots & \sigma_{1,n}^2 \\ \sigma_{2,1}^2 & \sigma_{2,2}^2 & \cdots & \sigma_{2,n}^2 \\ \vdots & \vdots & \ddots & \vdots \\ \sigma_{m,1}^2 & \sigma_{m,2}^2 & \cdots & \sigma_{m,n}^2 \end{bmatrix}.$$

In the variance–covariance matrix, the numbers on the left diagonal (i.e. from top-left to bottom-right) are variances, and the other numbers are the covariances between two variables. PCA can be defined as finding a matrix Y that can make $XX^{T}Y$ a diagonal matrix. The diagonal matrix is a matrix in which the entries outside of the left diagonal are all zero. By sorting the matrix Y in descending order of explainable variance, PCs are identified. These PCs can be expressed:

$$PC_n = a_{1,n}x_1 + a_{2,n}x_2 + \ldots + a_{m,n}x_m$$

https://doi.org/10.1017/S0016756821000418 Published online by Cambridge University Press

Table 1. Composition and textures of Wutonggou low-order cycle sandstones

			Grain composition (%)								Roundness	
Sample no.	Facies	Section	Q	F	Lv	Ls	M_z	SD	SK_i	K_G	ANLR (%)	RND (%)
S18-3	Fluvial lithic	ZBS	29	17	44	10	−0.13	0.46	0.12	1.45	63	37
gw9-10	Fluvial lithic	NTRL	7	32	54	8	0.67	1.27	−0.38	1.27	62	38
gw9-12	Fluvial lithic	NTRL	10	3	59	28	0.07	0.59	0.75	1.34	45	55
gw9-7	Fluvial lithic	NTRL	18	1	20	60	0.23	0.68	0.20	1.27	43	57
gw9-14	Fluvial lithic	NTRL	13	16	33	37	0.59	0.80	−0.26	1.16	33	67
GW9-17	Fluvial lithic	NTRL	3	6	50	41	−0.79	0.62	−0.08	1.17	30	70
Average			13	13	43	31	0.11	0.74	0.06	1.28	46	54
Median			12	11	47	32	0.15	0.65	0.02	1.27	44	56
S15-40	Fluvial feldspathic	ZBS	53	37	3	7	0.97	0.52	0.25	1.26	56	44
S15-53	Fluvial feldspathic	ZBS	20	43	30	7	1.00	0.50	0.09	1.28	62	38
S18-1	Fluvial feldspathic	ZBS	32	39	23	6	0.83	0.46	0.09	1.44	66	34
S18-2	Fluvial feldspathic	ZBS	26	39	27	8	1.22	0.50	0.05	1.29	66	34
S18-5	Fluvial feldspathic	ZBS	33	33	24	9	1.11	0.46	0.06	1.22	70	30
S18-6	Fluvial feldspathic	ZBS	24	39	28	8	1.59	0.57	−0.01	1.28	74	26
Average			31	38	23	7	1.12	0.50	0.09	1.29	66	34
Median			29	39	26	7	1.06	0.50	0.08	1.28	66	34
S15-33	Deltaic lithic	ZBS	48	13	21	18	−0.95	0.89	−0.15	1.14	31	69
S15-37	Deltaic lithic	ZBS	63	17	6	14	1.30	0.45	0.20	1.42	51	49
S15-48	Deltaic lithic	ZBS	51	7	12	30	−0.52	1.05	0.21	1.57	28	72
S15-52	Deltaic lithic	ZBS	38	23	23	16	0.04	0.87	0.33	1.44	46	54
TD168	Deltaic lithic	TDG	8	21	66	6	0.32	0.63	0.26	1.15	56	44
D4-17	Deltaic lithic	ZBS	10	17	48	29	0.31	0.68	0.13	1.07	30	70
SD12-16	Deltaic lithic	DLK	6	16	39	42	0.84	0.44	0.28	1.69	32	68
SD12-14	Deltaic lithic	DLK	18	21	36	33	0.55	0.39	0.23	1.80	45	55
D8-17	Deltaic lithic	DLK	10	6	36	51	−0.53	0.72	0.05	1.08	42	58
D9-17	Deltaic lithic	DLK	9	9	32	52	−0.02	0.78	0.56	1.44	30	70
D10-17	Deltaic lithic	DLK	6	35	36	25	1.12	0.50	0.15	1.24	50	50
Average			24	17	32	29	0.22	0.67	0.20	1.37	40	60
Median			10	17	36	29	0.31	0.68	0.21	1.42	42	58
S15-47	Deltaic feldspathic	ZBS	53	46	0	1	1.95	0.46	0.04	1.40	52	48
GW9-19	Deltaic feldspathic	NTRL	55	23	7	15	0.64	0.59	0.06	1.51	70	30
NTR36-17	Deltaic feldspathic	NTRL	49	27	6	18	1.77	0.50	−0.03	1.43	80	20
NTR37-17	Deltaic feldspathic	NTRL	56	29	2	13	1.98	0.44	0.09	1.27	60	40
Average			53	31	4	12	1.59	0.50	0.04	1.40	65	35
Median			54	28	4	14	1.86	0.48	0.05	1.41	65	35
S15-55	Littoral lithic	ZBS	32	30	26	12	1.03	0.55	0.21	1.27	53	47
S18-7	Littoral lithic	ZBS	23	37	28	12	1.38	0.60	0.00	1.43	81	19
TD5-17	Littoral lithic	TDG	0	10	65	25	2.33	0.73	0.01	1.18	49	51
TD151	Littoral lithic	TDG	3	5	69	23	−0.10	1.15	−0.34	0.88	59	41
TD157	Littoral lithic	TDG	12	19	59	10	1.25	0.88	−0.06	1.19	87	13
TD162	Littoral lithic	TDG	7	17	65	10	0.86	1.07	−0.07	1.02	70	30
TD174	Littoral lithic	TDG	7	9	48	36	−0.41	0.78	0.06	1.15	91	9

(*Continued*)

https://doi.org/10.1017/S0016756821000418 Published online by Cambridge University Press

Table 1. (*Continued*)

			Grain composition (%)								Roundness	
Sample no.	Facies	Section	Q	F	Lv	Ls	M_z	SD	SK_i	K_G	ANLR (%)	RND (%)
TD185	Littoral lithic	TDG	8	20	39	32	0.60	0.85	0.17	0.97	62	38
D1-17	Littoral lithic	DLK	12	21	30	40	−0.04	1.18	0.58	1.01	22	78
gw9-9	Littoral lithic	NTRL	12	14	35	39	0.02	0.80	0.84	1.12	39	61
GW9-15	Littoral lithic	NTRL	5	11	59	25	0.12	0.77	0.14	1.15	35	65
GW9-18	Littoral lithic	NTRL	9	28	49	14	1.06	0.67	0.24	1.22	59	41
NTR39-17	Littoral lithic	NTRL	20	34	14	22	1.15	0.48	0.05	1.28	62	38
Average			12	20	45	23	0.71	0.81	0.14	1.14	59	41
Median			9	19	48	23	0.86	0.78	0.06	1.15	59	41
S15-31	Littoral feldspathic	ZBS	55	32	6	7	0.76	0.58	−0.08	1.29	58	42
S15-35	Littoral feldspathic	ZBS	49	32	9	10	1.12	0.50	0.12	1.28	82	18
S15-36	Littoral feldspathic	ZBS	56	24	6	13	−0.11	0.78	−0.73	1.26	44	56
S15-38	Littoral feldspathic	ZBS	58	31	3	7	0.83	0.91	0.19	1.21	60	40
S15-41	Littoral feldspathic	ZBS	44	45	4	7	1.21	0.49	−0.04	1.38	72	28
S15-45	Littoral feldspathic	ZBS	64	21	4	11	0.01	0.51	0.82	1.37	48	53
S15-49	Littoral feldspathic	ZBS	49	41	3	7	1.28	0.48	−0.02	1.58	80	20
S15-51	Littoral feldspathic	ZBS	42	37	10	11	1.11	0.52	0.18	1.28	41	59
S15-59	Littoral feldspathic	ZBS	31	43	17	9	0.60	0.53	0.10	1.78	49	51
TD128	Littoral feldspathic	TDG	49	37	4	11	2.12	0.57	0.19	1.28	86	14
TD131	Littoral feldspathic	TDG	36	42	12	10	2.33	0.63	0.02	1.34	74	26
TD137	Littoral feldspathic	TDG	56	34	1	8	2.00	0.49	0.01	1.24	71	29
Average			49	35	6	9	1.10	0.58	0.06	1.36	64	36
Median			49	36	5	9	1.12	0.53	0.06	1.29	65	35

Q – quartz; F – feldspar; Lv – volcanic lithic; Ls – sedimentary lithic; M_z – graphic mean; SD – graphic standard deviation; SK_i – graphic skewness; K_G – graphic kurtosis; ANLR – angular grain; RND – rounded grain.

Table 2. Verbal limits of graphic mean, graphic standard deviation, skewness and kurtosis

Graphic mean Φ (mm)	Very fine	Fine	Medium	Coarse	Very coarse	
	3–4 (0.063–0.125)	2–3 (0.125–0.25)	1–2 (0.25–0.5)	0–1 (0.5–1)	−1–0 (1–2)	
Graphic standard deviation	Very well sorted	Well sorted	Moderately well sorted	Moderately sorted	Poorly sorted	Very poorly sorted
	< 0.35	0.35–0.5	0.5–0.7	0.7–1	1–2	2–4
Skewness	Very negative skewed	Negative skewed	Nearly symmetrical	Positive skewed	Very positive skewed	
	−1 to −0.3	−0.3 to −0.1	−0.1 to 0.1	0.1 to 0.3	0.3 to 1	
Kurtosis	Very platykurtic	Platykurtic	Mesokurtic	Leptokurtic	Very leptokurtic	Extremely leptokurtic
	< 0.67	0.67–0.9	0.9–1.11	1.11–1.5	1.5–3	> 3

The verbal limit of grain size follows the Udden–Wentworth grain size scale (Udden–Wentworth, 1992); the verbal limits of sorting, skewness and kurtosis follow Folk & Ward (1957).

where n is the component number, a the component loading, x the measured variable and m the total number of variables.

Before performing PCA, the data are standardized to remove the influences of fundamental units and to centre the dataset. Moreover, as PCA involves the variance–covariance matrix, the correlation coefficient, which is the division of the covariance by the roof of variance, can be calculated. The relationship between two variables can therefore be investigated.

4. Results

4.a. Textural characteristics of WTG-LC sandstones

A total of 52 WTG-LC sandstones are classified as fluvial, deltaic and littoral sandstone facies. Moreover, facies are further divided as lithic and feldspathic subfacies in terms of their composition (Tables 1, 3; online Supplementary Table S1). Accordingly, fluvial lithic sandstone, fluvial feldspathic sandstone, deltaic lithic

https://doi.org/10.1017/S0016756821000418 Published online by Cambridge University Press

Table 3. Compositional and textural characteristics of the various sandstone facies

		Fluvial sandstones		Deltaic sandstones		Littoral sandstones	
		FL	FF	DL	DF	LL	LF
Counts		6	6	11	4	13	12
Components (%)	Q	13	31	23	53	11	49
	F	13	38	17	31	18	35
	Lv	43	24	32	4	48	6
	Ls	31	7	28	12	23	9
M_z (Φ)	Mean	0.11	1.12	0.22	1.59	0.71	1.10
	Median	0.15	1.06	0.31	1.86	0.86	1.12
SD (Φ)	Mean	0.74	0.50	0.67	0.50	0.81	0.58
	Median	0.65	0.50	0.68	0.48	0.78	0.53
SK_i	Mean	0.06	0.09	0.20	0.04	0.14	0.06
	Median	0.02	0.08	0.21	0.05	0.06	0.06
K_G	Mean	1.28	1.29	1.37	1.40	1.14	1.36
	Median	1.27	1.28	1.42	1.41	1.15	1.29
Angular grains (%)	Mean	45	66	40	65	59	64
	Median	44	66	42	65	59	65
Rounded grains (%)	Mean	54	34	60	35	41	36
	Median	56	34	58	35	41	35

FL – fluival lithic; FF – fluvial feldspathic; DL – deltaic lithic; DF – deltaic feldspathic; LL – littoral lithic; LF – littoral feldspathic. See Table 1 or text for the rest of abbreviations.

sandstone, deltaic feldspathic sandstone, littoral lithic sandstone and littoral feldspathic sandstone are recognized. Textural characteristics, including graphic mean, graphic standard deviation, graphic skewness, kurtosis and degree of roundness are investigated for each subfacies (Figs 8, 9; Tables 1, 3). Comparisons are made following the order that the two subfacies from the same facies are compared first to investigate the influences of composition, then different facies but with similar composition are compared to explore the influences of depositional environments (Figs 8, 9; Tables 1, 3).

4.a.1. Fluvial lithic sandstones

Six fluvial lithic sandstones with quartz, feldspar, volcanic lithic and sedimentary lithic grains of 13%, 13%, 43% and 31%, respectively, are recognized. Overall, these sandstones are coarse-sized, moderately well to moderately sorted, nearly symmetrical skewed, leptokurtic and slightly rounded-grain dominant. The graphic mean ranges from 0.67Φ (0.63 mm) to −0.79Φ (1.73 mm), with an average of 0.11Φ (0.93 mm) and a median of 0.15Φ (0.90 mm). The graphic standard deviation varies from 0.46Φ to 1.27Φ, with an average of 0.74Φ and a median of 0.65Φ; the skewness varies from −0.38 to 0.75 with an average of 0.06 and a median of 0.02. The kurtosis ranges from 1.16 to 1.45 with an average of 1.28 and a median of 1.27. The sandstones contain 30–63% angular grains with an average of 45% and a median of 44%, and 37–70% rounded grains with an average of 54% and a median of 56% accordingly (Figs 8, 9; Table 3).

4.a.2. Fluvial feldspathic sandstones

Six fluvial feldspathic sandstones with quartz, feldspar, volcanic lithic and sedimentary lithic grains of 31%, 38%, 24% and 7%, respectively, have been recognized. These sandstones are overall coarse-sized, well sorted, nearly symmetrical skewed, leptokurtic and angular grain dominant. The graphic mean ranges from 1.59Φ (0.33 mm) to 0.83Φ (0.56 mm), with an average of 1.12Φ (0.46 mm) and a median of 1.06Φ (0.48 mm). The graphic standard deviation ranges from 0.46Φ to 0.57Φ, with an average of 0.50Φ and a median of 0.50Φ. The skewness varies from −0.01 to 0.25, with an average of 0.09 and a median of 0.08. The kurtosis ranges from 1.22 to 1.44, with an average of 1.29 and a median of 1.28. The sandstones contain 56–74% angular grains with an average of 66% and a median of 66%, and 26–44% rounded grains with an average of 34% and the median of 34%, accordingly (Figs 8, 9; Table 3).

4.a.3. Deltaic lithic sandstones

Eleven deltaic lithic sandstones with quartz, feldspar, volcanic lithic and sedimentary lithic grains of 23%, 17%, 32% and 28%, respectively, have been investigated. These sandstones are overall coarse-sized, moderately well sorted, positively skewed and leptokurtic, with dominant rounded grains. The graphic mean ranges from 1.30Φ (0.41 mm) to −0.95Φ (1.93 mm), with an average of 0.22Φ (0.86 mm) and a median of 0.31Φ (0.80 mm). The graphic standard deviation varies from 0.39Φ to 1.05Φ, with an average of 0.67Φ and a median of 0.68Φ. The skewness ranges from −0.15 to 0.56, with an average of 0.20 and a median of 0.21. The kurtosis ranges from 1.07 to 1.80, with an average of 1.37 and a median of 1.42. The sandstones contain 28–56% angular grains with an average of 40% and a median of 42%, and 44–72% rounded grains with an average of 60% and a median of 58% (Figs 8, 9; Table 3).

4.a.4. Deltaic feldspathic sandstones

Four deltaic feldspathic sandstones that consist of 53% quartz grains, 31% feldspar grains, 4% volcanic lithic grains and 12%

https://doi.org/10.1017/S0016756821000418 Published online by Cambridge University Press

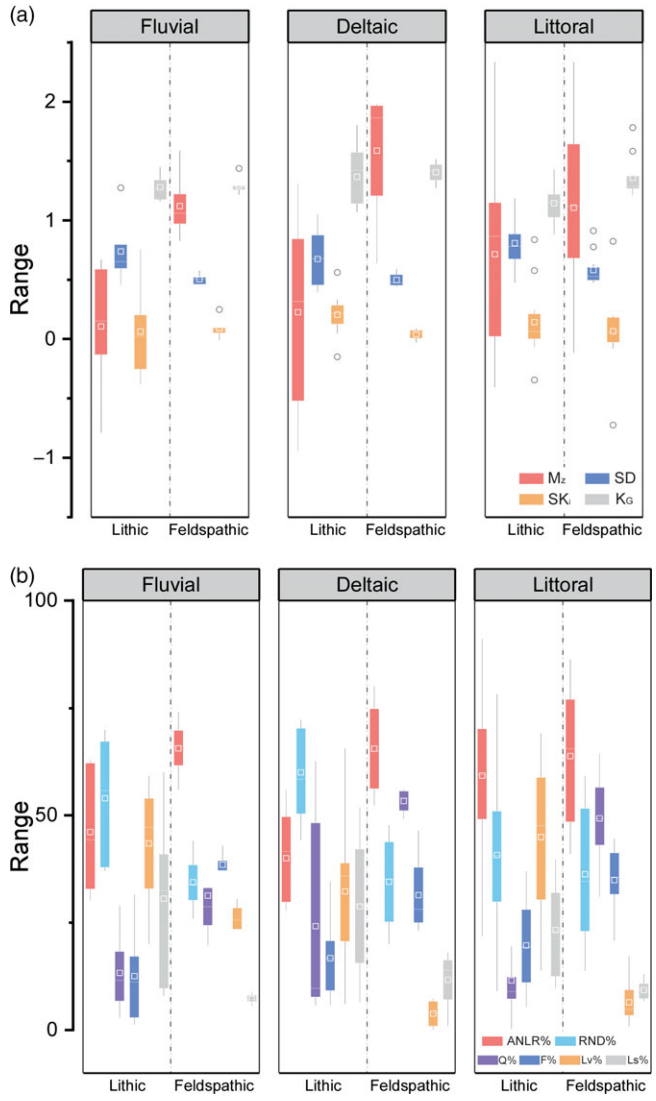

Fig. 8. (Colour online) Group box plots of textural and compositional data of Wutonggou low-order cycle sandstones. (a) Group box plots of graphic mean (M_z), graphic standard deviation (SD), skewness (SK_i) and kurtosis (K_G). The three columns are fluvial, deltaic and littoral sandstone facies, where the left columns in each facies are the lithic subfacies and the right columns are the feldspathic subfacies. (b) Group box plots of angular grain content (ANLR%), rounded grain content (RND%), quartz content (Q%), feldspar content (F%), volcanic lithic content (Lv%) and sedimentary lithic content (Ls%). White squares are median values, and the white dashed lines are the average. See text for abbreviations.

sedimentary lithic grains have been examined. These sandstones are dominantly medium-sized, well sorted, nearly symmetrical skewed, leptokurtic, and angular-grained. The graphic mean varies from 1.98Φ (0.25 mm) to 0.64Φ (0.64 mm), with an average of 1.59Φ (0.33 mm) and a median of 1.86Φ (0.28 mm). The graphic standard deviation changes from 0.44Φ to 0.59Φ, with an average of 0.50Φ and a median of 0.48Φ. The skewness varies from −0.03 to 0.09 with an average of 0.04 and a median of 0.05; the kurtosis ranges from 1.27 to 1.51 with an average of 1.40 and a median of 1.41. The total grains consist of 52–80% angular grains with an average of 65% and a median of 65%, and 20–48% rounded grains with an average of 35% and a median of 35% (Figs 8, 9; Table 3).

4.a.5. Littoral lithic sandstones

A total of 13 littoral lithic sandstones that have 11% quartz grains, 18% feldspar grains, 48% volcanic lithic grains and 23% sedimentary lithic grains have been studied. These sandstones are overall coarse-sized, moderately sorted, nearly symmetrical to positively skewed, leptokurtic and angular grain dominant. The graphic mean varies from 2.33Φ (0.20 mm) to −0.41Φ (1.32 mm), with an average of 0.71Φ (0.61 mm) and a median of 0.86Φ (0.55 mm). The graphic standard deviation changes from 0.48Φ to 1.18Φ, with an average of 0.81Φ and a median of 0.78Φ. The skewness varies from −0.34 to 0.84, with an average of 0.14 and a median of 0.06. The kurtosis ranges from 0.88 to 1.43, with an average of 1.14 and a median of 1.15. The total grains consist of 22–91% angular grains with an average of 59% and a median of 59%, and 9–78% rounded grains with an average of 41% and a median of 41% (Figs 8, 9; Table 3).

4.a.6. Littoral feldspathic sandstones

A total of 12 littoral feldspathic sandstones that consist of 49% quartz grains, 35% feldspar grains, 6% volcanic lithic grains and 9% sedimentary lithic grains have been investigated. These sandstones are overall medium-sized, moderately well sorted, nearly symmetrical skewed, leptokurtic and angular grain dominant. The graphic mean varies from 2.33Φ (0.20 mm) to −0.11Φ (1.08 mm), with an average of 1.10 Φ (0.46 mm) and a median of 1.12Φ (0.46 mm). The graphic standard deviation changes from 0.48Φ to 0.91Φ, with an average of 0.58 and a median of 0.53. The skewness varies from −0.73 to 0.82, with an average of 0.06 and a median of 0.06. The kurtosis ranges from 1.21 to 1.78, with an average of 1.36 and a median of 1.29. The total grains consist of 44–86% angular grains with an average of 64% and a median of 65%, and 14–56% rounded grains with an average of 36% and a median of 35% (Figs 8, 9; Table 3).

4.b. Comparisons among fluvial, deltaic and littoral facies

Textural characteristics are compared between the lithic and feldspathic sandstones of fluvial, deltaic and littoral facies (Figs 8, 9; Table 3). In this comparison, the textural differences reflect the influences of grain compositions. Moreover, different sandstone facies with similar composition are compared to investigate the influences of depositional environments (Figs 8, 9; Table 3).

4.b.1. Lithic and feldspathic sandstones

In addition to the large differences in composition between the lithic and feldspathic sandstones, the textural characteristics, including the graphic mean, graphic standard deviation and roundness, show significant differences.

The fluvial lithic sandstones are mainly coarse-sized, moderately sorted and have less angular grains than rounded grains; in contrast, the fluvial feldspathic sandstones are mostly medium-sized, well sorted and consist of more angular grains than rounded grains. Similarly, the deltaic lithic and deltaic feldspathic sandstones are also significantly different in grain size, sorting degree and roundness. The deltaic lithic sandstones are coarse-sized, moderately sorted and have less angular grains than rounded grains; in contrast, the deltaic feldspathic sandstones are medium- to coarse-sized, well sorted and have more angular grains than rounded grains. Regarding the littoral sandstones, the littoral lithic sandstones are coarse-sized and moderately sorted; on the contrary, the littoral feldspathic sandstones are medium-sized and well sorted.

https://doi.org/10.1017/S0016756821000418 Published online by Cambridge University Press

Table 4. Loadings of textural and compositional variables on PCs, explainable and cumulative explainable variance of PCs

	PC1	PC2	PC3	PC4	PC5	PC6	PC7	PC8	PC9	PC10
M_z	0.36	−0.11	0.25	−0.03	0.46	−0.36	0.49	0.47	0.00	0.00
SD	−0.28	−0.30	−0.44	0.23	−0.03	0.34	0.69	−0.03	0.00	0.00
SK_i	−0.11	0.35	0.52	0.71	0.09	0.28	0.08	−0.03	0.00	0.00
K_G	0.18	0.43	0.26	−0.52	−0.37	0.40	0.38	0.08	−0.02	0.00
ANLR (%)	0.35	−0.39	0.18	0.16	−0.40	−0.02	0.02	−0.10	0.01	0.71
RND (%)	−0.35	0.39	−0.18	−0.16	0.40	0.02	−0.02	0.10	−0.01	0.71
Q (%)	0.32	0.33	−0.44	0.27	−0.21	−0.03	−0.07	0.35	0.59	0.00
F (%)	0.41	0.01	−0.03	−0.09	0.45	0.20	0.07	−0.66	0.37	0.00
Lv (%)	−0.31	−0.41	0.32	−0.20	0.10	0.34	−0.17	0.30	0.59	0.00
Ls (%)	−0.38	0.13	0.20	−0.05	−0.25	−0.60	0.32	−0.33	0.41	0.00
Variance (%)	44	20	11	7	6	5	4	3	0	0
Cumulative variance (%)	44	64	75	82	88	93	97	100	100	100

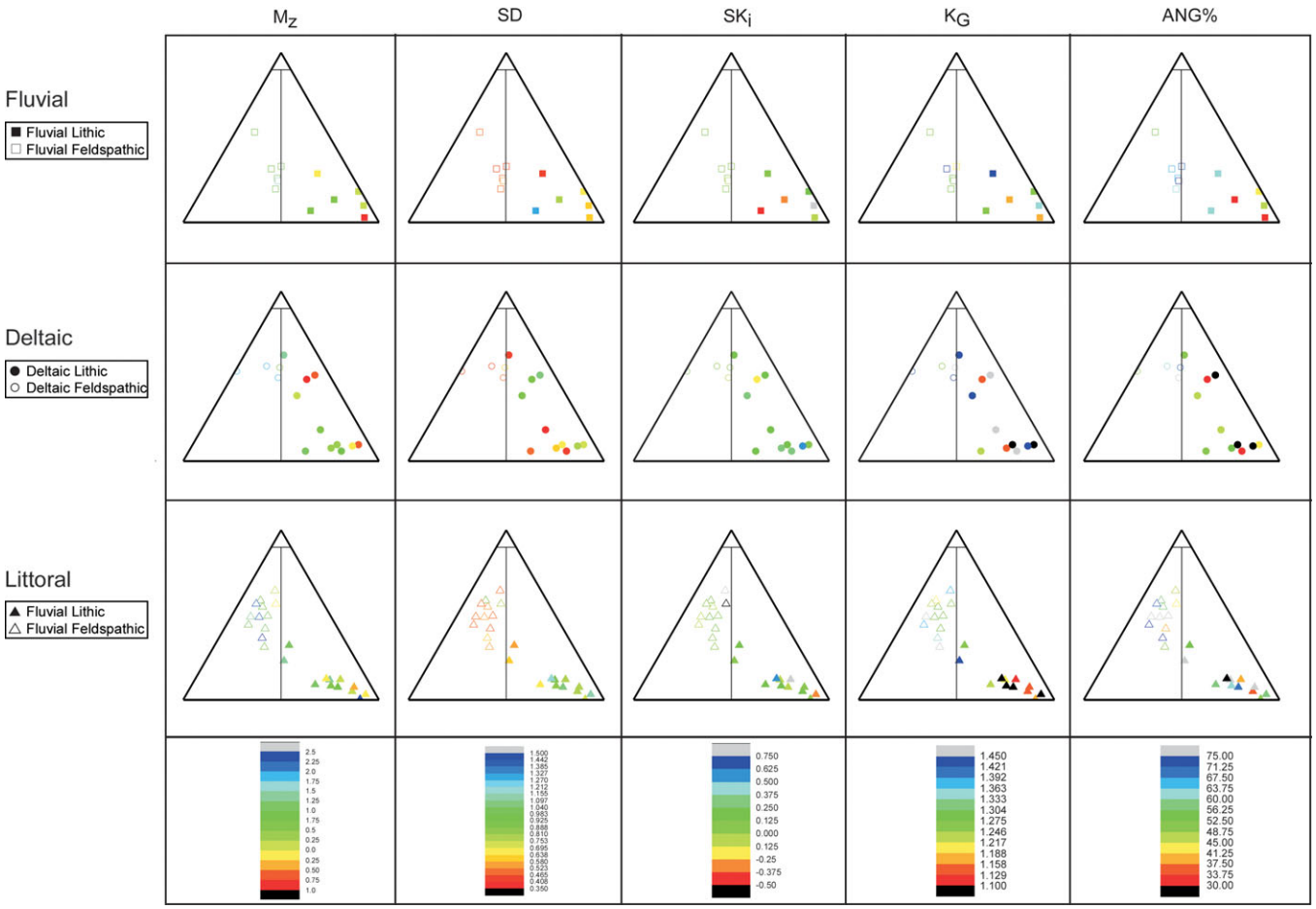

Fig. 9. (Colour online) Ternary diagrams of sandstones, showing the differences in textures between the lithic and feldspathic sandstones, and the differences among the fluvial, deltaic and littoral sandstones. The three ends in the ternary diagrams are quartz, feldspar and lithic fragments (the end-members in Fig. 7); the borders divided the quartz arenite, feldspathic sandstone and lithic sandstones as the divisions in Figure 7. See text for abbreviations.

4.b.2. Fluvial, deltaic and littoral sandstones

In contrast to the large differences in textural characteristics between lithic and feldspathic sandstones, sandstones of similar composition but derived from different depositional environments display null or negligible differences.

The fluvial lithic, deltaic lithic and littoral lithic sandstones show slight differences in roundness, and negligible differences in grain size and sorting degree. The only difference among these sandstones is that both fluvial and deltaic lithic sandstones contain less angular grains than rounded grains, but the littoral lithic

https://doi.org/10.1017/S0016756821000418 Published online by Cambridge University Press

sandstones have more angular grains. For the other textural characteristics, such as grain size and sorting degree, these sandstones have no major differences and are coarse-grained and moderately to moderately well sorted. Similarly, the fluvial feldspathic, deltaic feldspathic and littoral feldspathic sandstones also have limited variations in textures; these sandstones are mainly medium-sized, well sorted and contain more angular grains than rounded grains.

4.c. PCA results

PCA is performed with the standardized textural and compositional dataset (online Supplementary Table S2, available at http://journals.cambridge.org/geo). The first three components are the PCs that can explain 75% of the total variance of the whole dataset (Table 4).

The first principal component (PC1) accounts for 44% of the total variance. PC1 has a strong positive relationship with feldspar content, and moderate positive relationships with graphic mean and angular grain percentage (Table 4). Moreover, PC1 has moderate negative relationships with sedimentary lithic content, and rounded grain percentage. The second principal component (PC2) explains 20% of the total variance. PC2 has a strong positive relationship with kurtosis, a moderate positive relationship with rounded grain percentage, a strong negative relationship with volcanic lithic percentage, and a moderate negative relationship with angular grain percentage (Table 4). The third principal component (PC3) accounts for 11% of the total variance and has a relatively strong positive relation with skewness, and relatively strong negative relationships with graphic standard deviation and quartz content (Table 4).

In order to visualize the dataset on the new PCs coordinates, the dataset is plotted in two bivariate diagrams of PCs (Fig. 10). Fluvial lithic, fluvial feldspathic, deltaic lithic, deltaic feldspathic, littoral lithic and littoral feldspathic sandstones are labelled with different symbols in the bivariate plot. In these bivariate plots of PCs, sandstones are mainly divided into two groups along the horizontal axis. The fluvial, deltaic and littoral lithic sandstones are mainly placed in the left part of the plots, whereas the fluvial, deltaic and littoral feldspathic sandstones are mainly placed in the right part the plots. As the horizontal axis, namely PC1, is strongly related to feldspar and sedimentary lithic content, these two characteristics of sandstones are the best for grouping studied sandstones. On the contrary, fluvial, deltaic and littoral facies are not classified in these plots where different facies overlap without any clear divisions.

Moreover, the textural and compositional characteristics of these sandstones are correlative, which is indicated by the matrix of correlation coefficients (Fig. 11). The feldspar content has strong positive relationships with graphic mean and angular grain content, and strong negative relationships with lithic content, rounded grain content and graphic standard deviation. These correlations indicate that sandstone with a high content of feldspar grains is likely fine-grained and well sorted, and with scarce rounded, sedimentary and volcanic lithic grains. Moreover, the sedimentary lithic content has a strong positive relationship with rounded grain content, and strong negative relationships with angular grains, quartz content and graphic mean. These relationships indicate a sedimentary lithic-enriched sandstone, which usually contains many rounded and coarse grains. In addition to the correlation between composition and textures, textural features are also intercorrelated. Graphic mean has a strong positive relationship with angular grain content, and strong negative relationships with rounded grain content and graphic standard deviation. These relationships suggest that fine-grained sandstone contains more angular grains than rounded grains, and is usually well sorted.

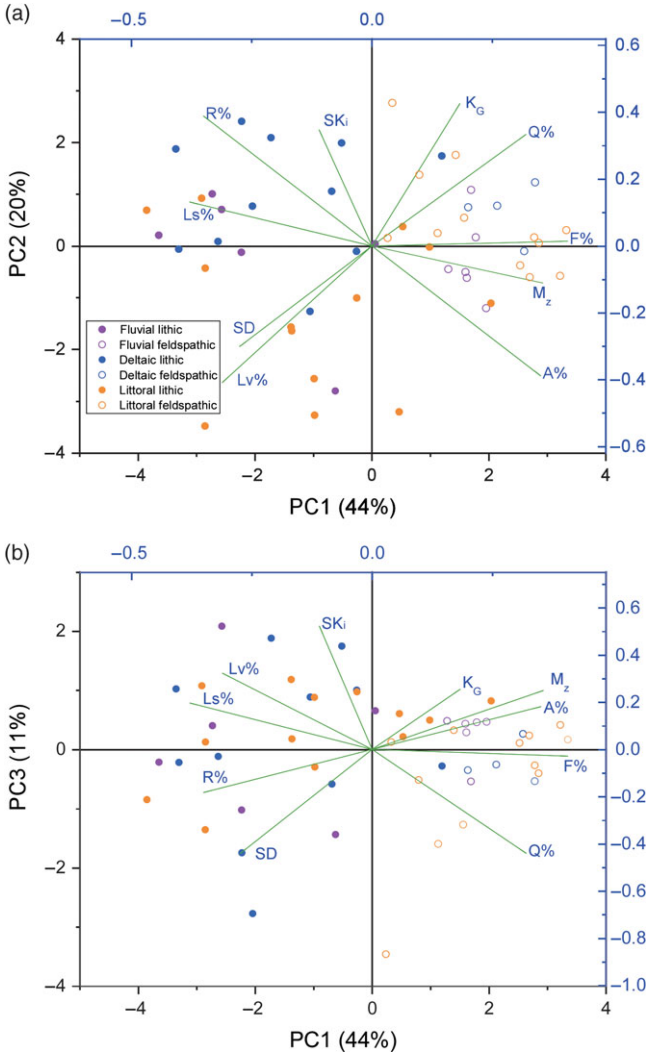

Fig. 10. (Colour online) Bivariate plots of (a) PC1 and PC2; and (b) PC1 and PC3. The projections of green lines along the axes of PCs indicate the relationship between this variable and the relevant PCs. The longer the projection, the stronger the relationship. The blue values are the correlation coefficients, and the black values are the data transformed under the new coordinates. See text for abbreviations.

5. Discussion

5.a. Provenance is the dominant control on sandstone textures

The large differences between the lithic and feldspathic sandstones suggest that provenance is the dominant controlling factor on texture. Sources of WTG-LC sandstones are interpreted from two major source regions with diverse source lithology. One source region is the Eastern North Tianshan Suture, which was covered with felsic-intermediate volcanic and plutonic rocks during late Permian – earliest Triassic time (Zheng, 2019; Zheng & Yang, 2020) and mainly supplied quartz, feldspar and volcanic lithic grains. The other source region is the local rift shoulders where old sedimentary rocks were exposed (Obrist-Farner & Yang, 2017; Zheng, 2019; Zheng & Yang, 2020) and provided a

https://doi.org/10.1017/S0016756821000418 Published online by Cambridge University Press

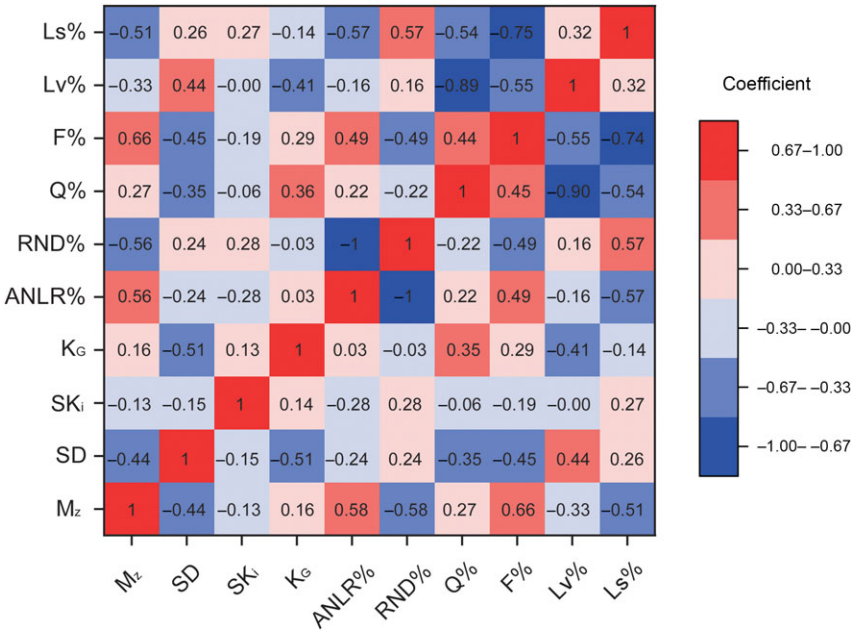

Fig. 11. (Colour online) Heat map of correlation coefficient of textural and compositional variables. The values on each grid are the coefficient between the two variables. Colour indicates the relationships; red represents a positive relationship and blue represents a negative relationship. Grids with darker colours indicate stronger relationships than the grids with lighter colours. See text for abbreviations.

sedimentary lithic source. Feldspathic sandstones consist of large amounts of quartz and feldspar grains, of which the sources are mainly fine-sized euhedral or subhedral quartz and feldspar phenocrysts in volcanic and plutonic rocks. In addition to their original fine size and high angularity, feldspar grains tend to be broken along their cleavages to form new grains during transportation (Odom, 1975; Morrone *et al.* 2018). As a result, feldspathic sandstones are overall medium-sized and contain abundant angular grains. In contrast to the source of quartz and feldspar phenocrysts, lithic grains, either from volcanic rocks in the suture zone or from the reworking sedimentary rocks, are much coarser in grain size (Morrone *et al.* 2020). Lithic sandstones are therefore coarser than feldspathic sandstones. Moreover, sedimentary rocks are labile and easily modified during transportation (Smith, 1972; Czerewko & Cripps, 2001). The angles on these grains are eroded to form the rounded sedimentary lithic grains. As well as grain size and degree of roundness, provenance also controls the sorting degree of sandstones. Sorting degrees are related to the overall grain sizes; finer-grained rocks, such as shale, have a better sorting degree than coarser-grained rocks, such as conglomerate (Folk & Ward, 1957). This relationship is also recognized in lithic and feldspathic WTG-LC sandstones. Feldspathic sandstones, which are finer-grained than lithic sandstones, are better sorted. Because provenance directly determines the grain sizes, the sorting degrees of sandstones are therefore indirectly controlled by provenance.

In contrast to provenance, the influence of depositional environments on sandstone textures is limited. Sandstones from different depositional settings show no distinct differences in textural characteristics. Moreover, the overlap of these sandstones in the PCA diagrams suggests that textural characteristics are incapable of classifying sandstones from different depositional settings. Although the oceanic beach sandstones are well differentiated from fluvial sandstones based on their good sorting degrees in published studies (e.g. Friedman, 1967), the good sorting degree is not unique for beach deposits; they are therefore not always well sorted (e.g. Solohub & Klovan, 1970; Alsharhan & El-Sammak, 2004; Anthony & Héquette, 2007). Similarly, littoral lithic sandstones of WTG-LC are not well sorted, and are not even better sorted than fluvial and deltaic sandstones. As discussed above, provenance greatly determines sandstone textures. Consequently, littoral lithic sandstones are better sorted than littoral feldspathic sandstones, despite being collected from the same depositional environments. Moreover, compared with marine environments, the lacustrine littoral zones are greatly influenced by river inflow, wave and current actions, and barely influenced by tides (Rust, 1982). Even the same lake in different localities or during various periods may receive different river flows with different intensities of waves. Moreover, as hummocky cross-stratifications are common in WTG-LC deposits (Yang *et al.* 2010), storm waves might redistribute the sediments by the removal and acquisition of clastics. Considering the influences of provenance, and the great heterogeneity in lakes, sandstone textures are good descriptive features but can be rather unreliable when classifying depositional environments.

5.b. The advantage of PCA in sandstone studies

Although Folk & Ward (1957) mentioned the problem that only one or two variables of sandstone texture can be investigated simultaneously, the most common methods of analysing sandstone textures currently still use either multiple independent diagrams to describe the characteristics or bivariate plots of two textural features to make comparisons. Obviously, a sandstone bears information that is incapable of being described in any single univariate or bivariate diagram. A good alternative to these traditional methods is the dimension reduction method, such as PCA. This method is an unsupervised machine-learning technique that has been applied in geological studies for decades (e.g. Hughes & Chapman, 1995; Pe-Piper *et al.* 2008). By transforming the coordinates of the raw dataset to find out the PCs that explain the highest variance, the important features can be extracted and the unnecessary information can be discarded. In this study, it is necessary to draw multiple ternary diagrams and box plots to distinguish these sandstones. However, only two PCA diagrams are required to group these sandstones: one group is quartz-,

https://doi.org/10.1017/S0016756821000418 Published online by Cambridge University Press

feldspar-, angular grain-enriched and well sorted; the other group is lithic grain- and rounded grain-enriched, and moderately to moderately well sorted. PCA might therefore be an excellent method for geologists to describe the rocks with limited efforts. Admittedly, PCA may also be incapable of correctly classifying samples in the case that the first few PCs cannot explain the majority of the variances of the dataset. This situation suggests that the samples either have no distinguishable pattern or require a more sensitive technique to classify them.

6. Conclusions

This study focuses on the textural characteristics of fluvio-lacustrine sandstones in the Bogda Mountains of NW China. Fluvial lithic, fluvial feldspathic, deltaic lithic, deltaic feldspathic, littoral lithic and littoral feldspathic sandstones are classified based on compositions and depositional environments.

The lithic and feldspathic sandstones from fluvial, deltaic and littoral environments are compared. It was found that the textural characteristics of lithic and feldspathic sandstones deriving from the same environment mainly differ in graphic mean, graphic standard deviation and roundness. On the contrary, sandstones from different depositional environments but with similar compositions have limited differences in textural characteristics. Moreover, three principal components (PCs) are recognized to explain 75% of the total variance of the dataset. PC1 can explain 44% of the total variance and is strongly related to the feldspar content. In the bivariate plots of PCs, WTG-LC sandstones can be classified based on their composition; that is, lithic and feldspathic sandstones are placed in different fields of the plots along the axis of PC1. However, sandstones from different depositional settings overlap and show no clear division. Moreover, textural and compositional characteristics are inter-correlated according to their correlation coefficients. Feldspar content is strongly related to graphic mean and angular grain content, and sedimentary lithic content is strongly related to rounded grain content.

The results of this study indicate that provenance, including the source lithology, original source size and mineralogy, is the most significant controlling factor for sandstone texture; in contrast, the influence of depositional environment on sandstone textures is limited. As well as highlighting the advantage of using PCA in sandstone studies, our study provides a detailed textural analysis of fluvio-lacustrine sandstones with complex provenance, and improves our understanding of the influences of provenance and depositional environment on sandstone textures.

Acknowledgements. We thank Dr Wan Yang of Missouri University of Science and Technology for his field assistance and discussions of the early draft, and Dr Obrist-Farner for his assistance with the petrographic study. We thank Dr Mingli Wan and Mr Shengwu Mei of Nanjing Institute of Geology and Paleontology of Chinese Academy of Sciences for their field assistance. We thank the associate editor Dr Stephen Hubbard, Dr Consuele Morrone and an anonymous reviewer for their constructive comments that greatly improved this manuscript. This research was partially supported by a contribution from the Alfred Spreng Graduate Research Grant from Geology and Geophysics Program of Missouri University of Science and Technology, National Science Foundation (grant no. IES-1714749) and National Natural Science Foundation of China (grant no. 42050104).

Declaration of interest. None.

Supplementary material. To view supplementary material for this article, please visit https://doi.org/10.1017/S0016756821000418

References

Alsharhan A and El-Sammak A (2004) Grain-size analysis and characterization of sedimentary environments of the United Arab Emirates coastal area. *Journal of Coastal Research* **20**(2), 464–77.

Anthony EJ and Héquette A (2007) The grain-size characterisation of coastal sand from the Somme estuary to Belgium: sediment sorting processes and mixing in a tide-and storm-dominated setting. *Sedimentary Geology* **202**, 369–82.

Arens S, Van Boxel J and Abuodha J (2002) Changes in grain size of sand in transport over a foredune. *Earth Surface Processes and Landforms* **27**, 1163–75.

Barndorff-Nielsen O (1977) Exponentially decreasing distributions for the logarithm of particle size. *Proceedings of the Royal Society of London. A. Mathematical and Physical Sciences* **353**, 401–19.

Boggs Jr S and Boggs S (2009) *Petrology of Sedimentary Rocks*. Cambridge: Cambridge University Press, 600 p.

Boulton G (1978) Boulder shapes and grain-size distributions of debris as indicators of transport paths through a glacier and till genesis. *Sedimentology* **25**, 773–99.

Charvet J, Shu L, Laurent-Charvet S, Wang B, Faure M, Cluzel D, Chen Y and De Jong K (2011) Palaeozoic tectonic evolution of the Tianshan belt, NW China. *Science China Earth Sciences* **54**, 166–84.

Czerewko M and Cripps J (2001) Assessing the durability of mudrocks using the modified jar slake index test. *Quarterly Journal of Engineering Geology and Hydrogeology* **34**, 153–63.

Davis JC and Sampson RJ (1986) *Statistics and Data Analysis in Geology*. New York: Wiley.

Dickinson WR (1970) Interpreting detrital modes of graywacke and arkose. *Journal of Sedimentary Research* **40**, 695–707.

Dickinson WR and Suczek CA (1979) Plate tectonics and sandstone compositions. *AAPG Bulletin* **63**, 2164–82.

Dott RH (1964) Wacke, graywacke and matrix; what approach to immature sandstone classification? *Journal of Sedimentary Research* **34**(3), 625–32.

Ehrlich R and Full W (1987) Sorting out geology—unmixing mixtures. In *Use and Abuse of Statistical Methods in Earth Sciences* (ed. WB Size), pp. 33–46. New York: Oxford University Press.

Folk RL (1980) *Petrology of Sedimentary Rocks*. Austin, TX: Hemphill Publishing Company, 190 p.

Folk RL and Ward WC (1957) Brazos River bar [Texas]; a study in the significance of grain size parameters. *Journal of Sedimentary Research* **27**, 3–26.

Fredericks JG (2017) Provenance and depositional environments of fluvial-lacustrine deposits in a non-marine rift basin, Lower-Triassic Jiucaiyuan and Shaofanggou low-order cycles Bogda Shan, NW China. M.Sc. thesis. Missouri University of Science and Technology, USA. Published thesis, 276 p.

Friedman GM (1962) On sorting, sorting coefficients, and the lognormality of the grain-size distribution of sandstones. *The Journal of Geology* **70**, 737–53.

Friedman GM (1967) Dynamic processes and statistical parameters compared for size frequency distribution of beach and river sands. *Journal of Sedimentary Research* **37**, 327–54.

Garzanti E (2016) From static to dynamic provenance analysis—sedimentary petrology upgraded. *Sedimentary Geology* **336**, 3–13.

Greene TJ, Carroll AR, Wartes M, Graham SA and Wooden JL (2005) Integrated provenance analysis of a complex orogenic terrane: Mesozoic uplift of the Bogda Shan and inception of the Turpan-Hami Basin, NW China. *Journal of Sedimentary Research* **75**, 251–67.

Guan W (2011) Provenance analysis of Upper Permian-basal Triassic fluvial lacustrine sedimentary rocks in the greater Turpan-Junggar Basin, southern Bogda Mountains, NW China. M.Sc. Thesis. Wichita State University, USA. Published thesis, 102 p.

Hughes NC and Chapman RE (1995) Growth and variation in the Silurian proetide trilobite Aulacopleura konincki and its implications for trilobite palaeobiology. *Lethaia* **28**, 333–53.

Ingersoll RV, Bullard TF, Ford RL, Grimm JP, Pickle JD and Sares SW (1984) The effect of grain size on detrital modes: a test of the Gazzi-Dickinson point-counting method. *Journal of Sedimentary Research* **54**, 103–16.

Johnsson MJ (1993) The system controlling the composition of clastic sediments. In *Processes Controlling the Composition of Clastic Sediments* (eds MJ Johnsson and A Basu), pp. 1–20. Boulder: Geological Society of America, Special Paper no. 284.

Krumbein WC and Sloss LL (1951) Stratigraphy and sedimentation. *Soil Science* **71**, 401.

Luplin JH and Hampson GJ (2020) Sediment-routing controls on sandstone bulk petrographic composition and texture across an ancient shelf: Example from Cretaceous Western Interior Basin, Utah and Colorado, U.S.A. *Journal of Sedimentary Research* **90**, 1389–09.

Mardia KV, Kent JT and Bibly JM (1979) *Multivariate Analysis*. London: Academic Press.

Marsaglia K and Ingersoll R (1992) Compositional trends in arc-related, deep-marine sand and sandstone: a reassessment of magmatic-arc provenance. *GSA Bulletin* **104**, 1637–49.

Morrone C, Le Pera E, De Rosa R and Marsaglia KM (2018) Beach sands of Lipari island, Aeolian archipelago: roundness study. *Rediconti Online Societa Geologica Italiana* **45**, 141–6.

Morrone C, Le Pera E, Marsaglia KM and De Rosa R (2020) Compositional and textural study of modern beach sands in the active volcanic area of the Campania region (southern Italy). *Sedimentary Geology* **396**, 105567.

Obrist-Farner J and Yang W (2015) Nonmarine time-stratigraphy in a rift setting: an example from the Mid-Permian lower Quanzijie low-order cycle, Bogda Mountains, NW China. *Journal of Palaeogeography* **4**, 27–51.

Obrist-Farner J and Yang W (2017) Provenance and depositional conditions of fluvial conglomerates and sandstones and their controlling processes in a rift setting, mid-Permian lower and upper Quanzijie low order cycles, Bogda Mountains, NW China. *Journal of Asian Earth Sciences* **138**, 317–40.

Odom IE (1975) Feldspar-grain size relations in Cambrian arenites, upper Mississippi Valley. *Journal of Sedimentary Research* **45**, 636–50.

Passega R (1957) Texture as characteristic of clastic deposition. *AAPG Bulletin* **41**, 1952–84.

Pe-Piper G, Triantafyllidis S and Piper DJ (2008) Geochemical identification of clastic sediment provenance from known sources of similar geology: the Cretaceous Scotian Basin, Canada. *Journal of Sedimentary Research* **78**, 595–607.

Pettijohn FJ, Potter PE and Siever R (1972) *Sand and Sandstone*. Berlin, Heidelberg, New York: Springer, 553 p.

Rust BR (1982) Sedimentation in fluvial and lacustrine environments. *Hydrobiologia* **91**, 119–45.

Shao L, Stattegger K and Garbe-Schoenberg C-D (2001) Sandstone petrology and geochemistry of the Turpan basin (NW China): implications for the tectonic evolution of a continental basin. *Journal of Sedimentary Research* **71**, 37–49.

Shu L, Wang B, Zhu W, Guo Z, Charvet J and Zhang Y (2011) Timing of initiation of extension in the Tianshan, based on structural, geochemical and geochronological analyses of bimodal volcanism and olistostrome in the Bogda Shan (NW China). *International Journal of Earth Sciences* **100**, 1647–63.

Smith ND (1972) Flume experiments on the durability of mud clasts. *Journal of Sedimentary Research* **42**, 378–83.

Solohub J and Klovan J (1970) Evaluation of grain-size parameters in lacustrine environments. *Journal of Sedimentary Research* **40**, 81–101.

Suttner LJ (1974) Sedimentary petrographic provinces: an evaluation. In *Paleogeographic Provinces and Provinciality* (ed. CA Ross), pp. 75–84. Tulsa: Society of Economic Paleontologists and Mineralogists, Special Publication no. 21.

Thomas SG, Tabor NJ, Yang W, Myers TS, Yang Y and Wang D (2011) Palaeosol stratigraphy across the Permian–Triassic boundary, Bogda Mountains, NW China: implications for palaeoenvironmental transition through earth's largest mass extinction. *Palaeogeography, Palaeoclimatology, Palaeoecology* **308**, 41–64.

Visher GS (1969) Grain size distributions and depositional processes. *Journal of Sedimentary Research* **39**, 1074–106.

Wartes MA, Carroll AR and Greene TJ (2002) Permian sedimentary record of the Turpan-Hami basin and adjacent regions, northwest China: constraints on postamalgamation tectonic evolution. *Geological Society of America Bulletin* **114**, 131–52.

Wentworth CK (1922) A scale of grade and class terms for clastic sediments. *The Journal of Geology* **30**, 377–92.

XBGMR (Xinjiang Bureau of Geology and Mineral Resources) (1993) *Regional Geology of the Xinjiang Uygur Autonomous Region*. Beijing: Ministry of Geology and Mineral Resources, Geological Memoirs, Series 1, No. 32. (in Chinese with English abstract).

Xia LQ, Xu XY, Xia ZC, Li XM, Ma ZP and Wang LS (2004) Petrogenesis of Carboniferous rift-related volcanic rocks in the Tianshan, northwestern China. *Geological Society of America Bulletin* **116**, 419–33.

Xiao WJ, Zhang LC, Qin KZ, Sun S and Li JL (2004) Paleozoic accretionary and collisional tectonics of the Eastern Tianshan (China): implications for the continental growth of central Asia. *American Journal of Science* **304**, 370–95.

Yang W, Feng Q, Liu Y, Tabor N, Miggins D, Crowley JL, Lin J and Thomas S (2010) Depositional environments and cyclo- and chronostratigraphy of uppermost Carboniferous–Lower Triassic fluvial-lacustrine deposits, southern Bogda Mountains, NW China: a terrestrial paleoclimatic record of mid-latitude NE Pangea. *Global and Planetary Change* **73**, 15–113.

Yang W, Liu Y, Feng Q, Lin J, Zhou D and Wang D (2007) Sedimentary evidence of Early–Late Permian mid-latitude continental climate variability, southern Bogda Mountains, NW China. *Palaeogeography, Palaeoclimatology, Palaeoecology* **252**, 239–58.

Zheng D (2019) Provenance and depositional environments of the upper Permian-lowermost Triassic fluvial and lacustrine sandstones, Wutonggou low-order cycle, Bogda Mountains, NW China. Ph.D. thesis, Department of Geology and Geophysics, Missouri University of Science and Technology, USA. Published thesis, 171 p.

Zheng DY and Yang W (2020) Provenance of upper Permian-lowermost Triassic sandstones, Wutonggou low-order cycle, Bogda Mountains, NW China: implications on the unroofing history of the Eastern North Tianshan Suture. *Journal of Palaeogeography* **9**, 1–21.

https://doi.org/10.1017/S0016756821000418 Published online by Cambridge University Press